Rashba effect in quantum networks

Dario Bercioux[1,2], Michele Governale[3], Vittorio Cataudella[2], and Vincenzo Marigliano Ramaglia[2]
[1] *Institut für Theoretische Physik, Universität Regensburg, D-93040, Germany*
[2] *Coherentia-INFM & Dipartimento di Scienze Fisiche Università degli Studi "Federico II", I-80126 Napoli, Italy*
[3] *NEST-INFM & Scuola Normale Superiore, Piazza dei Cavalieri 7, I-56126 Pisa, Italy*

(Dated: November 12, 2018)

We present a formalism to study quantum networks made up by single-channel quantum wires in the presence of Rashba spin-orbit coupling and magnetic field. In particular, linear transport through one-dimensional and two-dimensional finite-size networks is studied by means of the scattering formalism. In some particular quantum networks, the action of the magnetic field or of the Rashba spin-orbit coupling induces localization of the electron wave function. This phenomenon, which relies on both the quantum-mechanical interference and the geometry of the network, is manifested through the suppression of the conductance for specific values of the spin-orbit-coupling strength or of the magnetic field. Furthermore, the interplay of the Aharonov-Bohm phases and of the non-Abelian phases, introduced by spin-orbit coupling, is discussed in a number of cases.

PACS numbers: 73.23.-b,73.20.Fz,72.25.-b

I. INTRODUCTION

In recent years, a effect of extreme localization induced by magnetic field has been predicted in a class of two-dimensional rhombus tilings[1]. This effect is related to the interplay between the Aharonov-Bohm (AB) effect[2] and the geometry of the network. For special values of the perpendicular magnetic field, the set of sites visited by an initially localized wave packet is bounded by the AB destructive interference. This set of sites is referred to as *AB cage*. This kind of localization does not requires the presence of disorder[3], as it relies on quantum-interference and on the geometry of the lattice. There have been several theoretical works addressing different aspects of AB cages, as the effect of disorder and electron-electron interaction[4], interaction induced delocalization[5], transport[6], and realizations in fully frustrated superconducting systems[7,8].

Two series of experiments have confirmed the existence of the AB-cage effect. Abilio *et al.*[9] have shown that a $\mathcal{T}_3$ network realized with superconducting wires exhibits a striking reduction of the critical current and of the superconducting transition temperature for the predicted values of the magnetic field. Naud *et al.*[10] have measured megnetoresistance oscillations of a normal $\mathcal{T}_3$ network, tailored in a high mobility two-dimensional electron gas (2DEG).

It is known that a wavefunction on an electron moving in the presence of Spin-Orbit (SO) coupling acquires quantum phases due to the Aharonov-Casher effect[11,12,13,14,15,16]. We focus on the Rashba SO coupling[17,18], which is present in semiconductor heterostructures due to lack of inversion symmetry in growth direction. It is usually important in small-gap zinc–blende–type semiconductors, and its strength can be tuned by external gate voltages. This has been demonstrated experimentally measuring the Shubnikov-de Haas oscillations [19,20,21,22] or antiweak localization[23] in two-dimensional electron gases.

In a recent Letter[24], it has been shown that in a linear chain of square loops connected at one vertex (termed *diamond chain*), localization of the electron wavefunction can be obtained by means of the Rashba effect.

In this paper the formalism introduced in our previous work[24] is extended to include both Rashba SO coupling and magnetic field. In this case, electrons traveling in the network acquire both the AB phase factors and the non-Abelian phases induced by SO coupling. The main aim of the present paper is to study the interplay of the magnetic field and of the SO coupling, and to investigate two-dimensional networks with Rashba SO coupling (previously only one-dimensional networks were studied).

The paper is organized in the following way. In Sec. II we introduce the model and the formalism used to study a quantum network realized with single-channel quantum wires in the presence of Rashba SO coupling and of an external magnetic field. Section III is devoted to the transport properties of one-dimensional networks in the presence of magnetic field and Rashba SO coupling. In Sec. IV results for transport through two-dimensional networks are presented. Conclusions are drawn at the end of the paper.

II. MODEL AND FORMALISM

We consider a two-dimensional network (in the xy plane) made up of single-channel quantum wires with Rashba SO coupling, and we allow for the presence of a magnetic field perpendicular to the plane of the network.

We start from the Hamiltonian of a single-channel wire along a generic direction $\hat{\gamma}$ in the xy plane:

$$\mathcal{H} = \frac{(p_\gamma + qA_\gamma)^2}{2m} + \frac{\hbar k_{\mathrm{SO}}}{m}\left(p_\gamma + qA_\gamma\right)\left(\hat{\gamma}\times\hat{z}\right)\cdot\vec{\sigma}, \quad (1)$$

where m is the electron effective mass, $\vec{A}$ the vector potential, and k_{SO} the SO coupling strength. The SO coupling strength k_{SO} is related to the spin precession length

$L_{\rm SO}$ by $L_{\rm SO}=\pi/k_{\rm SO}$. For InAs quantum wells the spin-precession length ranges from 0.2 to 1 μm[19,20,21,22,23]. We neglect the Zeeman splitting introduced by the magnetic field. The wavefunction on a bond (quantum wire) connecting two generic nodes α and β along the direction $\hat{\gamma}_{\alpha\beta}$ reads

$$\mathbf{\Psi}_{\alpha\beta}(r)=\frac{e^{-if_{\alpha r}}e^{-i(\hat{\gamma}_{\alpha\beta}\times\hat{z})\cdot\vec{\sigma}\ k_{\rm SO}r}}{\sin(kl_{\alpha\beta})}\left\{\sin\left[k(l_{\alpha\beta}-r)\right]\mathbf{\Psi}_\alpha\right.$$
$$\left.+\sin(kr)e^{if_{\alpha\beta}}e^{i(\hat{\gamma}_{\alpha\beta}\times\hat{z})\cdot\vec{\sigma}\ k_{\rm SO}l_{\alpha\beta}}\mathbf{\Psi}_\beta\right\}. \quad (2)$$

where k is related to the eigen energy by $\epsilon=\frac{\hbar^2}{2m}(k^2-k_{\rm SO}^2)$, r is the coordinate along the bond, and $l_{\alpha\beta}$ the length of the bond[25]. The magnetic field gives rise to the phase factors

$$\exp\{-if_{\alpha,r}\}=\exp\left\{-i\frac{2\pi}{\phi_0}\int_\alpha^r\vec{A}\cdot\mathrm{d}\vec{l}\right\}, \quad (3)$$

where $\phi_0=h/e$ is the flux quantum. The spinors $\mathbf{\Psi}_\alpha$ and $\mathbf{\Psi}_\beta$ are the values of the wavefunction at the nodes α and β respectively. The spin precession due to the Rashba effect is described by the exponentials containing Pauli matrices in Eq. (2).

Equation (2) is the key step to generalize the existing methods to study quantum networks[6,24,26] in the presence of Rashba SO coupling and magnetic field. The wavefunction of the whole network is obtained by imposing the conservation of probability current at every node. For a generic node α it reads:

$$\mathbf{M}_{\alpha\alpha}\mathbf{\Psi}_\alpha+\sum_{\langle\alpha,\beta\rangle}\mathbf{M}_{\alpha\beta}\mathbf{\Psi}_\beta=0, \quad (4)$$

where

$$\mathbf{M}_{\alpha\alpha} = \sum_{\langle\alpha,\beta\rangle}\cot kl_{\alpha\beta} \quad (5a)$$

$$\mathbf{M}_{\alpha\beta} = -\frac{e^{-if_{\alpha\beta}}e^{i(\hat{\gamma}_{\alpha\beta}\times\hat{z})\cdot\vec{\sigma}\ k_{\rm SO}l_{\alpha\beta}}}{\sin kl_{\alpha\beta}}. \quad (5b)$$

In Eqs. (4) and (5) the sum $\sum_{\langle\alpha,\beta\rangle}$ runs over all nodes β which are connected by a bond to the node α. This set of boundary conditions ensures the self-adjointness of the Schrödinger operator for the whole network.

For a closed network, the secular equation is derived requiring a non-trivial solution for the set of equations obtained writing the condition Eq. (4) at every node. A similar approach, making use of the Bloch condition, can be used for computing the spectrum of an infinite periodic network.

In this paper, we are mainly concerned in calculating linear transport through a finite-size network connected to external leads. The linear conductance can be evaluated making use of the Landauer–Büttiker scattering formalism[27,28]. We proceed along the lines proposed by Vidal *et al.*[6]. Here, we describe the method for the case of only two external leads; a generalization to many leads is straightforward. In the two output/input semi-infinite leads, we assume that there is no SO coupling, and no magnetic field. To compute the transmission coefficients we inject from the input wire an electron with spin $\sigma=\pm$ along a generic direction, whose corresponding spinors are χ_σ. The wavefunctions on the external leads are simply

$$\Psi_{\rm in}(r) = e^{ik_{\rm in}r}\chi_\sigma+\sum_{\sigma'}r_{\sigma'\sigma}e^{-ik_{\rm in}r}\chi_{\sigma'} \quad (6)$$

$$\Psi_{\rm out}(r) = \sum_{\sigma'}t_{\sigma'\sigma}e^{ik_{\rm in}r}\chi_{\sigma'}, \quad (7)$$

where r is the coordinate on the semi-infinite input/output lead, with the origin fixed at the position of the input/output node. The transmission and reflection coefficients ($t_{\sigma'\sigma}$ and $r_{\sigma'\sigma}$, respectively) can be obtained by solving the linear system of equations arising from the continuity of the probability current at all nodes in the network, and of the wavefunction at the input and output nodes. The conditions for the continuity of the probability current at internal nodes are given in Eq. (4). For the external nodes they read

$$\mathbf{M}_{00}\mathbf{\Psi}_0+\sum_{\langle 0,\beta\rangle}\mathbf{M}_{0\beta}\mathbf{\Psi}_\beta=-i(\chi_\sigma-\sum_{\sigma'}r_{\sigma'\sigma}\chi_{\sigma'}) \quad (8)$$

$$\mathbf{M}_{NN}\mathbf{\Psi}_N+\sum_{\langle N,\beta\rangle}\mathbf{M}_{N\beta}\mathbf{\Psi}_\beta=i\sum_{\sigma'}t_{\sigma'\sigma}\chi_{\sigma'}, \quad (9)$$

where the injection node is labeled as "0" and the output node as "N". The total transmission coefficient is then simply $|t|^2=\sum_{\sigma,\sigma'}|t_{\sigma'\sigma}|^2$.

We now introduce some concepts useful for understanding the interference phenomena due to magnetic field and Rashba SO coupling. Let us suppose that an electron is at node α with a spinor $\mathbf{\Psi}_\alpha$ and that it travels along the bond from α to β. When it reaches node β it has acquired a phase. Its spinor in β is related to the one in α by

$$\mathbf{\Psi}_\beta=R_{\rm dyn}(l_{\alpha\beta},k)R_{\rm AB}(\alpha,\beta)\mathbf{R}_{\rm SO}(\alpha,\beta)\mathbf{\Psi}_\alpha, \quad (10)$$

The dynamical phase is simply $R_{\rm dyn}(l_{\alpha\beta},k)=\exp(ikl_{\alpha\beta})$. The AB phase is

$$R_{\rm AB}(\alpha,\beta)=\exp\left\{-i\frac{2\pi}{\phi_0}\int_\alpha^\beta\vec{A}\cdot\mathrm{d}\vec{l}\right\}. \quad (11)$$

The SO coupling, on the other hand, introduces a non-Abelian phase (a rotation in spin space), which reads

$$\mathbf{R}_{\rm SO}(\alpha,\beta)=\exp\left[-i(\hat{\gamma}_{\alpha\beta}\times\hat{z})\cdot\vec{\sigma}\ k_{\rm SO}l_{\alpha\beta}\right]. \quad (12)$$

Equation (10) can be used to understand the difference between the interference induced by an AB phase and a non-Abelian phase. Let us consider a rhombus-like loop. An electron is injected at one of the vertices and collected at the opposite one. The phase (10) acquired by

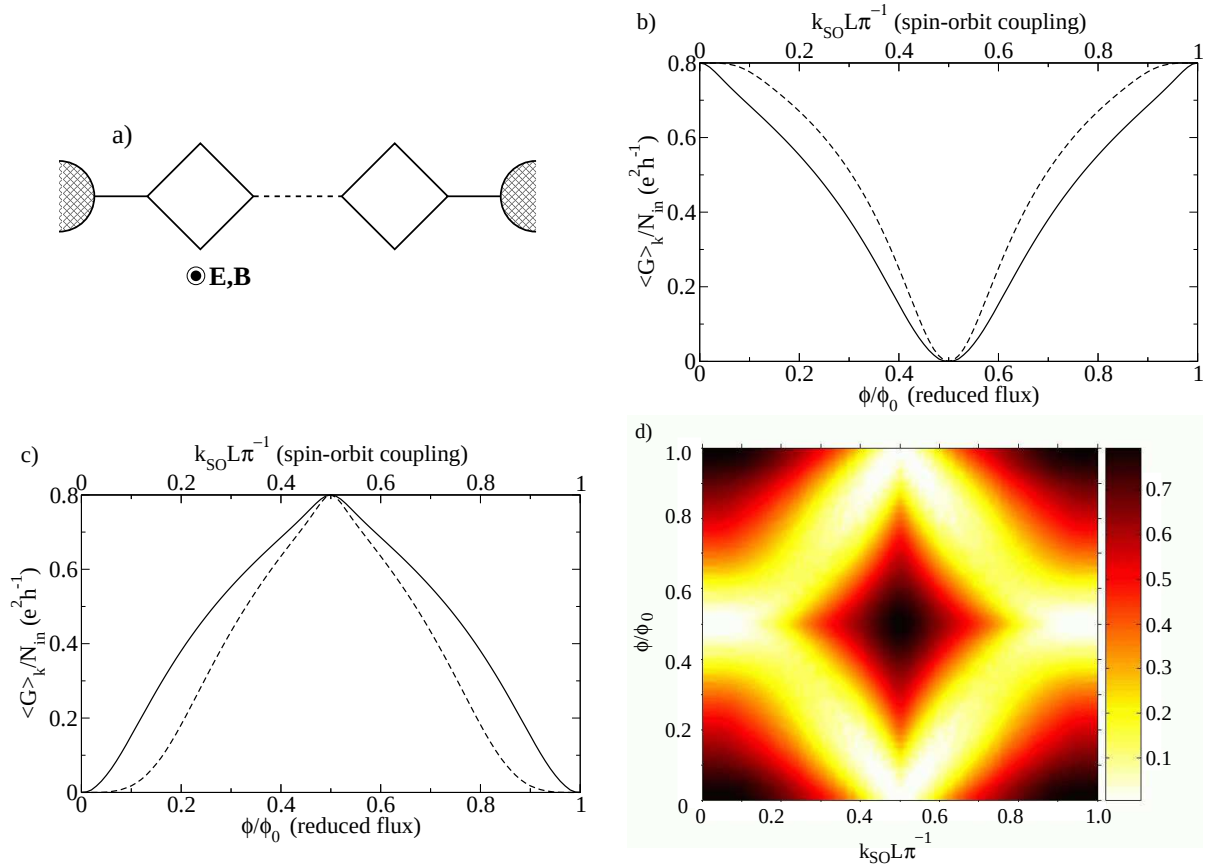

FIG. 1: (color online) Panel a): A finite-size piece of the diamond chain connected to reservoirs. There are 1 input and 1 output single-channel leads. The number of input channels, considering spin, is $N_{\rm in} = 2$.
Panel b): Averaged conductance per channel, $\langle G\rangle_k/N_{\rm in}$, as a function of the reduced flux (solid line) evaluated at $k_{\rm SO}L\pi^{-1} = 0$, and of spin-orbit coupling evaluated at $\phi/\phi_0 = 0$ (dashed line) for the diamond chain with 10 elementary squares.
Panel c): Averaged conductance per channel, $\langle G\rangle_k/N_{\rm in}$, as a function of the reduced flux evaluated at $k_{\rm SO}L\pi^{-1} = 0.5$ (solid line), and of spin-orbit coupling evaluated at $\phi/\phi_0 = 0.5$ (dashed line).
Panel d): Color-scale plot of the averaged conductance $\langle G\rangle_k$ as a function of the reduced flux and spin-orbit coupling.

the electron wavefunction is different along the two possible paths. Destructive interference is achieved only when the two partial waves for these paths sum to zero at the final point. A straightforward calculation shows that it is possible to obtain destructive interference induced by the AB phase in every rhombus-like loop. Instead, the non-Abelian phase Eq. (12), gives rise to destructive interference only for the special case of a square.

III. ONE-DIMENSIONAL NETWORKS

In this section we study linear transport through one-dimensional networks. In particular we consider a *diamond chain* [shown in panel a) of Fig. 1], i.e a chain of squares connected at one vertex, and a square ladder [shown in panel a) of Fig. 2].

The diamond chain is a bipartite structure containing nodes with different coordination numbers. For the diamond chain, electron localization due to SO coupling has been demonstrated in Ref. 24. Here, we study the interplay of SO coupling and of an orbital magnetic field. The conductance is a function of the injection wave-vector $k_{\rm in}$, and it is periodic in $k_{\rm in}$ with period π/L, being L the length of a bond. Furthermore, the conductance as a function of $k_{\rm in}$ shows a rich interference pattern. As we are not interested in the interference due to the dynamical phases $R_{\rm dyn}$, we have made the usual choice [see Ref. 6] to integrate the conductance over $k_{\rm in} \in [0, \pi/L]$. Throughout this paper, the integrated conductance will be indicated by $\langle G\rangle_k$. We note that finite temperature or finite voltage will introduce in a natural way an average over $k_{\rm in}$. For $\mathrm{Max}[K_{\rm B}T, eV] \geq K_{\rm B}T^* = \frac{\hbar^2}{m}k_F\frac{\pi}{L}$, $\langle G\rangle_k$ will be the quantity measured in the transport experiments. Taking for the Fermi energy of the single-channel wires 10 meV, $m/m_e = 0.042$ for the effective mass (InAs), and $L = 1\mu$m, yields $T^* \approx 7$ K.

In panel b) of Fig. 1, we show the conductance $\langle G\rangle_k$ as a function of the reduced flux for zero SO coupling (solid line), and as a function of the SO-coupling strength

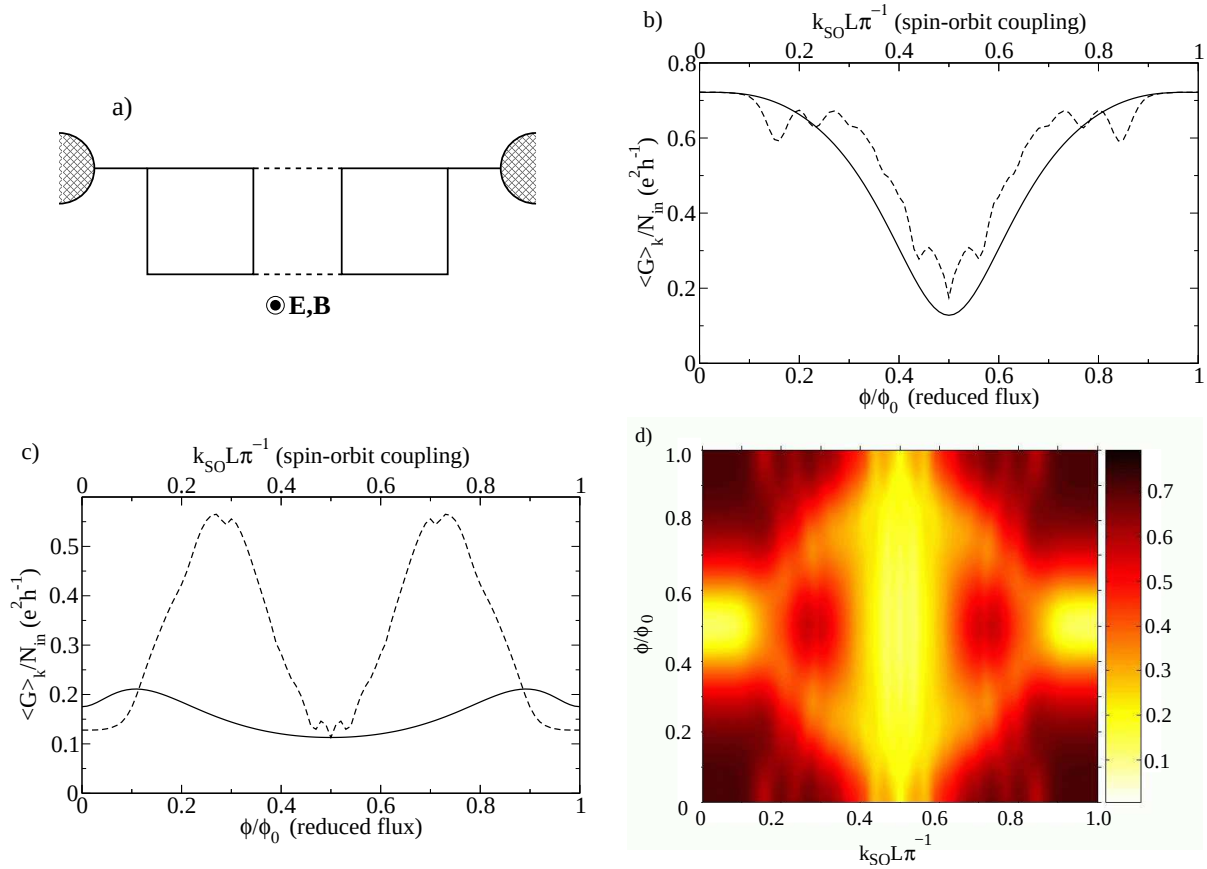

FIG. 2: (color online) Panel a): A finite-size piece of the square ladder connected to reservoirs. There are 1 input and 1 output single-channel leads. The number of input channels, considering spin, is $N_{\rm in} = 2$.
Panel b): Averaged conductance per channel, $\langle G\rangle_k/N_{\rm in}$, as function of the reduced flux (solid line), and of spin-orbit coupling (dashed line) for the ladder with 10 elementary squares.
Panel c): Averaged conductance per channel, $\langle G\rangle_k/N_{\rm in}$, as function of the reduced flux evaluated at $k_{\rm SO}L\pi^{-1} = 0.5$ (solid line), and of spin-orbit coupling evaluated at $\phi/\phi_0 = 0.5$ (dashed line).
Panel d): Color-scale plot of the averaged conductance $\langle G\rangle_k$ as a function of the reduced flux and spin-orbit coupling.

for zero magnetic field (dashed line). The reduced flux is defined as the number of flux quanta per unit rhombus. In this geometry, when either magnetic field or SO coupling is present, the integrated conductance reaches zero both as a function of the reduced flux (zero SO coupling) and as a function of SO coupling strength (zero magnetic field). In the first case the conductance vanishes when the reduced flux is a half integer, in the latter when $k_{\rm SO}L/\pi$ is a half integer. One can easily prove, making use of Eq. (10), that the vanishing conductance is due to the full interference of the partial waves traveling on the upper and lower arm of a diamond. In such a situation electron localization is achieved. Depending on the mechanism which leads to localization, this effect is called AB-cage effect or Rashba-cage effect.

It is interesting to study the combined effect of the magnetic field and of the SO coupling. This is done in panel c) of Fig. 1, where the conductance $\langle G\rangle_k$ is plotted as a function of the SO coupling for $\phi/\phi_0 = 0.5$ (dashed line), and as function of the magnetic field for $k_{\rm SO}L\pi^{-1} = 0.5$ (solid line). Let us concentrate on the fixed-SO-coupling case (solid line): when the reduced flux is 0 or 1, we are in a condition of complete interference induced by the SO coupling; when the flux is moved away from these values, the AB phase changes and the interference is no more fully destructive. This give rise to the typical anti-localization peak shown in panel c). A very similar analysis applies to the fixed-flux case (dashed line). The full dependence of the conductance $\langle G\rangle_k$ on both the reduced flux and SO coupling is shown, as a color-scale plot, in panel d) of Fig. 1. The anti-localization peak is clearly visible in the center of the plot.

Disorder is inevitable in nanostructures and its effect needs to be accounted for. From previous studies, both the Rashba-cage effect and the AB-cage effect are expected to be robust against disorder. We consider a model where the length of each bond is randomly distributed in the interval $[L - \Delta L, L + \Delta L]$, and we average observable quantities over disordered configurations.

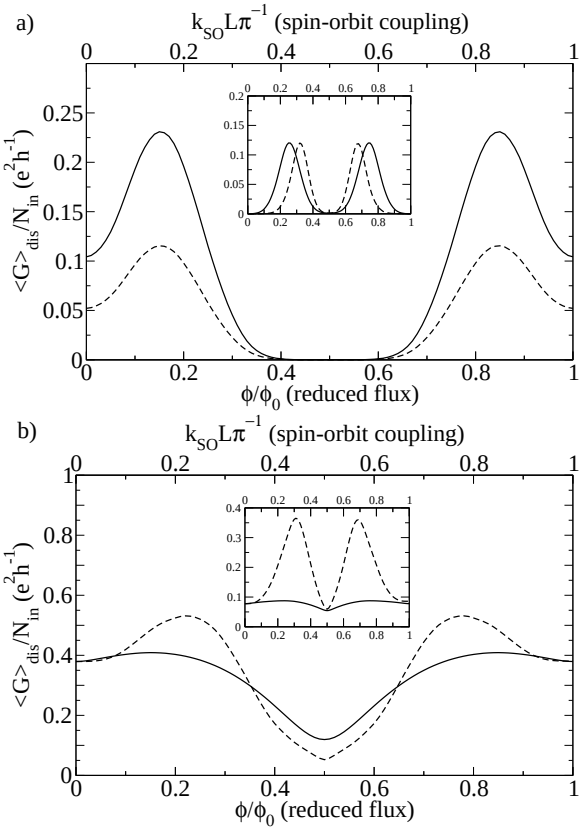

FIG. 3: Panel a): Disorder-averaged conductance per channel, $\langle G\rangle_{dis}/N_{\rm in}$, as function of the reduced flux for zero spin-orbit coupling (solid line), and of spin-orbit coupling for zero magnetic field (dashed line), for the diamond chain with 10 elementary squares.
Panel b): Disorder-averaged conductance per channel, $\langle G\rangle_{dis}/N_{\rm in}$, as function of the reduced flux for zero spin-orbit coupling (solid curve), and of spin-orbit coupling for zero magnetic field (dashed curve), for the ladder with 10 elementary squares.
In both panels, the injection wave-vector is uniformly distributed in $[k_{\rm F}-\frac{\pi}{2L}, k_{\rm F}+\frac{\pi}{2L}]$ with $k_{\rm F}L = 100$, and the disorder strength is $\Delta L/L = 0.01$ for the main panel, and $\Delta L/L = 0.05$ for the inset.

The half width of the distribution ΔL gives the strength of the disorder. This type of disorder is particularly dangerous because it affects the phases acquired by electrons when traveling along the bonds. We consider the physical situation $\Delta L/L \ll 1$. Under this condition the dispersion of loop areas is negligible, and the periodicity with reduced flux is preserved. Consistently, we neglect the effect of the bond-length fluctuations on the AB phases[6].

In the absence of disorder, the conductance is periodic in the flux ϕ/ϕ_0 and in $k_{\rm SO}L/\pi$ with periodicity 1. Increasing disorder the periodicity with magnetic field and spin-orbit will be eventually halved. The halving of the oscillation period is due to the Altshuler-Aronov-Spivak (AAS) effect[29], and it is related to the enhancement of back-reflection due to interference of pair of paths traveling clockwise and counter-clockwise along a square of the chain (according to weak localization picture). A detailed study of the period-halving transition as a function of disorder strength for the $\mathcal{T}_3$ lattice with magnetic field, has been presented in Ref. 6. Our findings agree with the scenario presented there.

The disordered-average conductance for the diamond chain is shown in panel a) of Fig. 3. For moderate-strength disorder ($k_{\rm F}\Delta L \approx 1$) we find both the AB- and the Rashba-cage effect are preserved. Only at higher disorder strengths [see the inset of panel a)] the halving of the periodicity takes place.

The square ladder has a complete different topology and this is reflected in its transport properties. In particular, no localization is expected to occur. In Fig. 2 and in panel b) of Fig.3, for the sake of comparison, the same quantities displayed previously for the diamond chain, are shown for the square ladder. The main results being that no localization occurs, and that in the presence of disorder AAS oscillation are present.

IV. TWO-DIMENSIONAL SYSTEMS

We now turn our attention to two-dimensional networks. In particular, we consider transport through a finite piece of $\mathcal{T}_3$ lattice and contrast it with transport through a finite piece of square lattice. The way the finite-size networks are connected to reservoirs, kept at different chemical potentials, is shown in panel a) of Figs. 4 and 5.

The $\mathcal{T}_3$ lattice [shown in panel a) of Fig. 4] is a periodic hexagonal structure with three sites per unit cell, one sixfold coordinated and two threefold coordinated. This is an example of two-dimensional regular bipartite lattice containing nodes with different coordination numbers .

We show that in this kind of structure transport properties exhibit a signature of the interference effects due to Rashba SO coupling and to magnetic field. In fact we expect complete localization by means of magnetic field[6], but not of Rashba SO coupling, as can be predicted by considering interference of partial waves with the phase factors given in Eq. (10).

In panel b) of Fig. 4, we show the conductance $\langle G\rangle_k$ through a finite piece of $\mathcal{T}_3$ lattice, as a function of the reduced flux for zero SO coupling (solid line), and as a function of the SO-coupling strength for zero magnetic field (dashed line). When the SO coupling is absent we observe a suppression of the conductance at half-integer values of the reduced flux, due to the existence of the AB-cage effect. The residual value of the conductance minimum is not zero due to the existence of dispersive edge states[30]. This residual value is independent of the number of injection channels. On the other hand, when the magnetic field is absent we do not observe such a strong suppression of the conductance as a function of the SO coupling. A minimum is still present, but this is due to partial interference, which does not induce com-

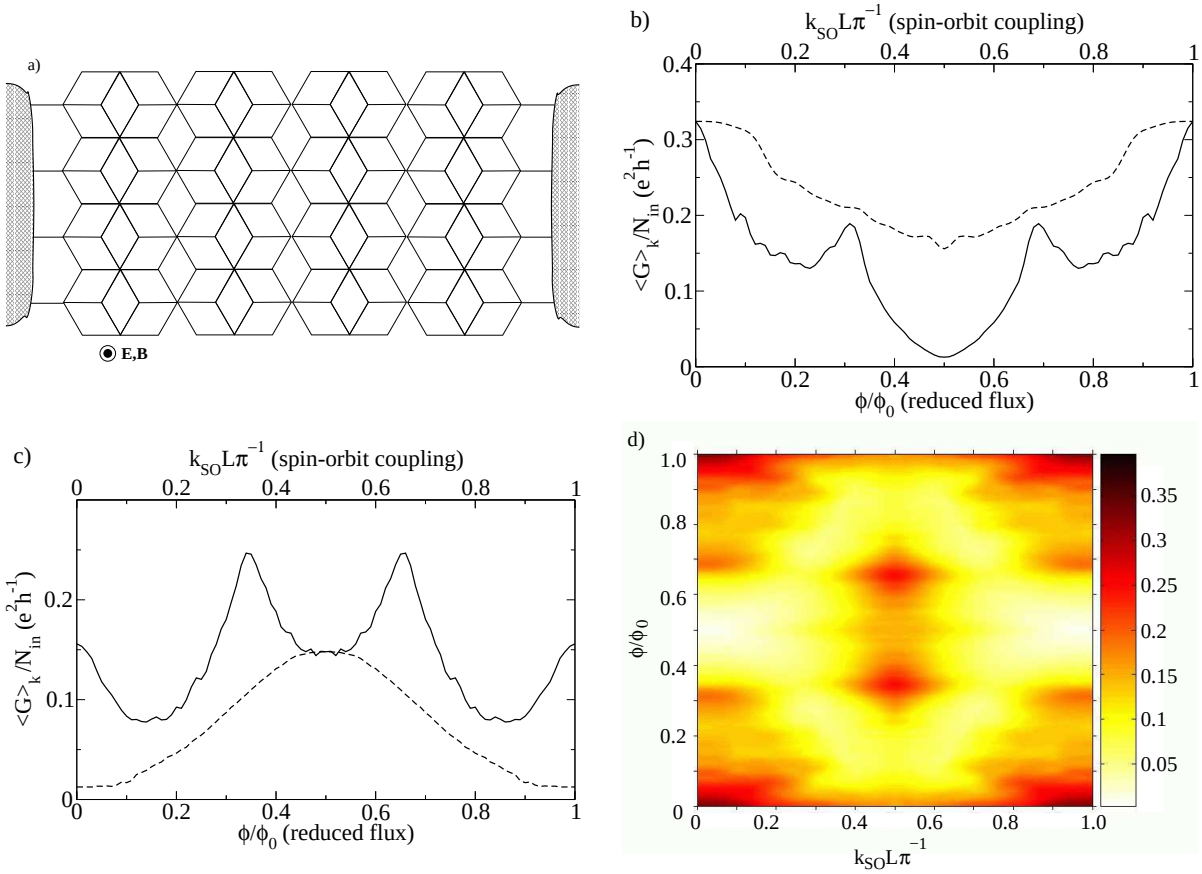

FIG. 4: (color online) Panel a): A finite-size piece of the $\mathcal{T}_3$ network connected to reservoirs. There are 4 input and 4 output single-channel leads. The number of input channels, considering spin, is $N_{\rm in} = 8$.
Panel b): Averaged conductance per channel, $\langle G\rangle_k/N_{\rm in}$, as a function of the reduced flux evaluated at $k_{\rm SO}L\pi^{-1} = 0$ (solid line), and of spin-orbit coupling evaluated at $\phi/\phi_0 = 0$ (dashed line) for the $\mathcal{T}_3$ lattice with 200 quantum wires (89 rhombi).
Panel c): Averaged conductance per channel, $\langle G\rangle_k/N_{\rm in}$, as a function of the reduced flux evaluated at $k_{\rm SO}L\pi^{-1} = 0.5$ (solid line), and of spin-orbit coupling evaluated at $\phi/\phi_0 = 0.5$ (dashed line).
Panel d): Color-scale plot of the averaged conductance per channel, $\langle G\rangle_k/N_{\rm in}$, as a function of the reduced flux and spin-orbit coupling.

plete localization. Furthermore, the finite conductance at the minimum cannot be attributed to the existence of edge states, because its value depends on the number of injection channels.

In panel c) of Fig. 4, we show the conductance $\langle G\rangle_k$ as a function of the SO coupling for $\phi/\phi_0 = 0.5$ (dashed line), and as a function of the magnetic field with $k_{\rm SO}L\pi^{-1} = 0.5$ (solid line). In the case of fixed finite SO coupling, the behavior of the conductance as a function of reduced flux is qualitatively similar to when the SO coupling is absent. In particular, a well defined minimum for $\phi/\phi_0 = 0.5$ is still observed. On the other hand, for fixed magnetic field, the SO coupling suppresses the destructive interference due to the AB effect and an anti-localization peak takes place. Panel d) of Fig. 4 shows the full dependence of the conductance $\langle G\rangle_k$ as a function of both reduced flux and SO coupling.

In panel a) of Fig. 6 we show the behavior of the disorder-averaged conductance as a function of the reduced flux (solid line) for zero SO coupling, and as function of the SO coupling (dashed line) for zero magnetic field. The periodicity of the disorder-averaged conductance as function of $k_{\rm SO}L/\pi$ is no longer 1 but 1/2. The oscillation with period 1 have been washed out, while those with period 1/2 are still present since they are related to phase-coherent pairs of time reversed trajectories according to the weak-localization pictures. This is consistent with the fact that in the $\mathcal{T}_3$ the SO coupling does not induce complete localization, and therefore, the oscillation with period 1 are not protected against disorder. On the other hand, the disorder-averaged conductance as a function of the reduced flux remains, for this disorder strength, still ϕ_0-periodic.

We now consider transport through a finite-size square lattice [shown in panel a) of Fig. 5]. This network, unlike the $\mathcal{T}_3$ lattice, does not fulfill the necessary condition to exhibit the AB- or Rashba-cage effect, i.e. it does not present a bipartite structure containing nodes with different coordination numbers. Accordingly, we do not expect any electron localization phenomenon caused ei-

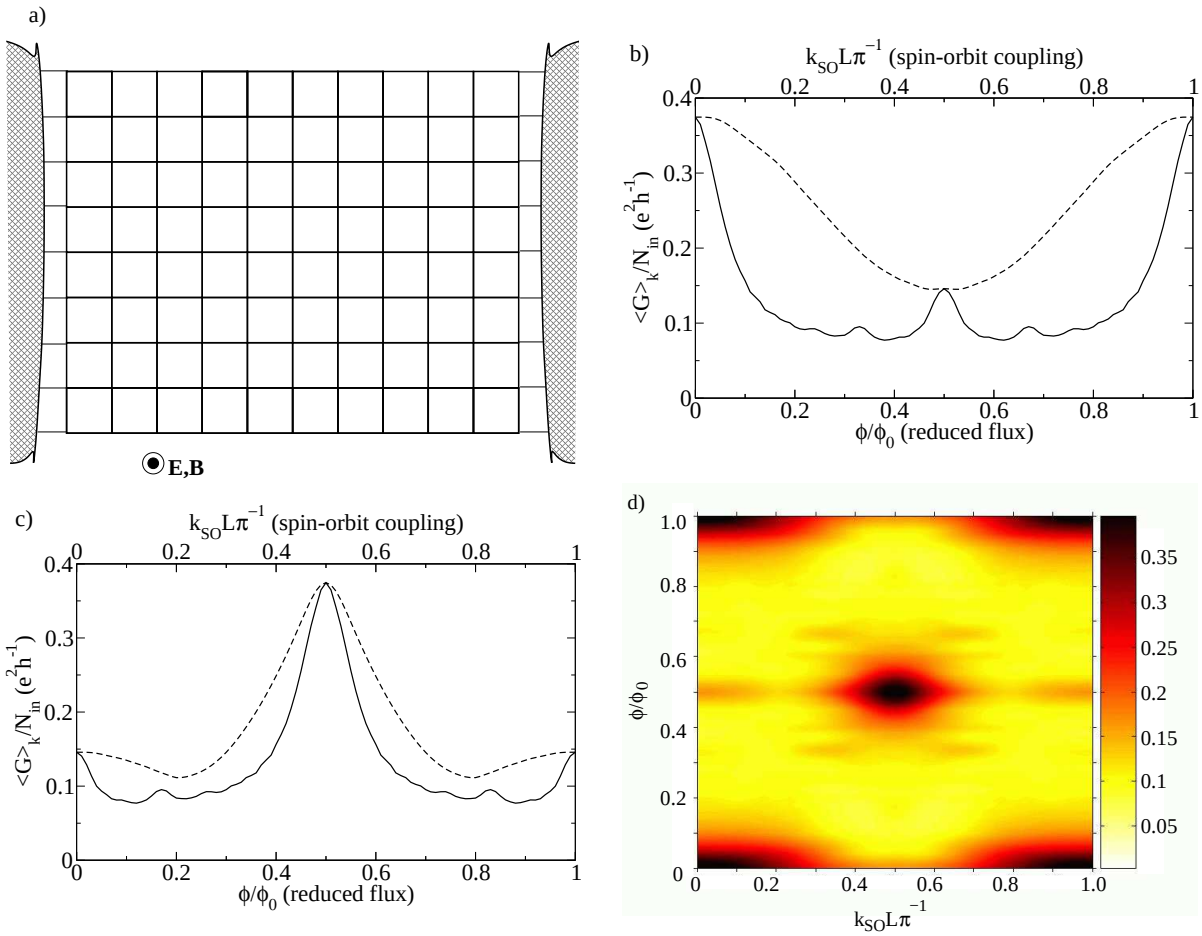

FIG. 5: (color online) Panel a): A finite-size piece of the square lattice connected to reservoirs. There are 9 input and 9 output single-channel leads. The number of input channels, considering spin, is $N_{\rm in} = 18$.
Panel b): Averaged conductance per channel, $\langle G\rangle_k/N_{\rm in}$, as a function of the reduced flux evaluated at $k_{\rm SO}L\pi^{-1} = 0$ (solid line), and of spin-orbit coupling evaluated at $\phi/\phi_0 = 0$ (dashed line) for the square lattice with 178 quantum wires (80 squares).
Panel c): Averaged conductance per channel, $\langle G\rangle_k/N_{\rm in}$, as a function of the reduced flux evaluated at $k_{\rm SO}L\pi^{-1} = 0.5$ (solid line), and of spin-orbit coupling evaluated at $\phi/\phi_0 = 0.5$ (dashed line).
Panel d): Color-scale plot of the averaged conductance per channel, $\langle G\rangle_k/N_{\rm in}$, as a function of the reduced flux and spin-orbit coupling.

ther by the magnetic field or the SO coupling.

In panel b) of Fig.5, we show the conductance $\langle G\rangle_k$ through a finite-size square lattice as a function of the reduced flux for zero SO coupling (solid line), and as a function of the SO-coupling strength for zero magnetic field (dashed line). The overall behavior of the conductance as a function of magnetic field (zero SO coupling) and of SO coupling (zero magnetic field) is very different. However it has to be noticed that both curves reach the same value, respectively, at $\phi/\phi_0 = 1/2$ (solid line) and $k_{\rm SO}L\pi^{-1} = 1/2$ (dashed line). It is interesting to analyze what happens when both the magnetic field and the SO coupling are present. In panel c) of Fig. 4, we show the conductance $\langle G\rangle_k$ as a function of the SO coupling for $\phi/\phi_0 = 0.5$ (dashed line), and as a function of the magnetic field with $k_{\rm SO}L\pi^{-1} = 0.5$ (solid line). The behavior of both curves is very similar. In particular, the conductance shows an anti-localization-like peak both as a function of SO coupling and of magnetic field, respectively, around $\phi/\phi_0 = 0.5$ and $k_{\rm SO}L\pi^{-1} = 0.5$. The full dependence of the conductance $\langle G\rangle_k$ as a function of both reduced flux and SO coupling is shown in panel d) of Fig. 5, where it can be seen that significative conductance is obtained only in the anti-localization peak at the center of the plot.

In panel b) of Fig. 6, we show the disorder-averaged conductance as a function of the reduced flux (solid line) for zero SO coupling, and as function of the SO coupling (dashed line) for zero magnetic field. In this case, we notice that the oscillations of period 1 as a function of magnetic field are more robust than those as a function of SO coupling (but not as robust as in the $\mathcal{T}_3$ when localization is achieved).

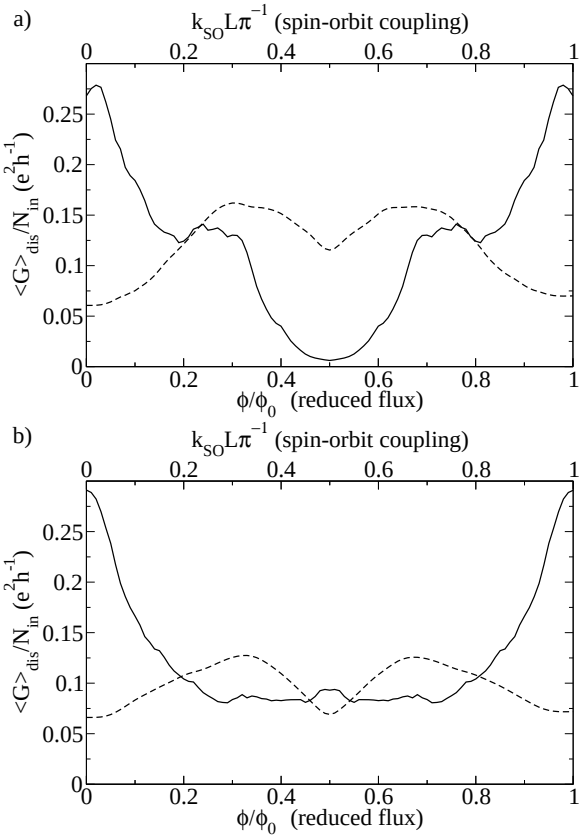

FIG. 6: Panel a) Disorder-averaged conductance per channel, $\langle G\rangle_{dis}/N_{\rm in}$, as a function of the reduced flux (solid line), and of spin-orbit coupling (dashed line), for the $\mathcal{T}_3$ lattice with 200 quantum wires (89 rhombi).
Panel b) Disorder-averaged conductance per channel, $\langle G\rangle_{dis}/N_{\rm in}$, as a function of the reduced flux (solid line) and of spin-orbit coupling (dashed line), for the square lattice with 178 quantum wires (80 squares).
In both panels, the injection wave-vector is uniformly distributed in $[k_{\rm F}-\frac{\pi}{2L}, k_{\rm F}+\frac{\pi}{2L}]$ with $k_{\rm F}L = 100$, and the disorder strength is $\Delta L/L = 0.05$.

V. CONCLUSION

We have introduced a formalism to study quantum networks made by single-channel quantum wires in the presence of Rashba spin-orbit coupling and of magnetic field. In particular, we have investigated the interplay of the AB phases and of the non-Abelian phases introduced by SO coupling in transport through finite-size one-dimensional and two dimensional networks.

While SO coupling can induce localization in particular one-dimensional networks[24], complete localization by means of SO coupling has not been found in the two-dimensional $\mathcal{T}_3$ lattice. However, signatures of the SO coupling are still visible in the transport properties, and intriguing effects occur due to the presence of both magnetic field and SO coupling.

Acknowledgments

Fruitful discussions with C. Cacciapuoti, G. De Filippis, P. Lucignano and C.A. Perroni (*Federico II* University, Naples, Italy) and with R. Fazio, D. Frustaglia and M. Rizzi (*Scuola Normale Superiore*, Pisa, Italy) are gratefully acknowledged. Finally DB wishes to acknowledge A. Ceré (*Hippos Campi Flegrei*, Naples, Italy).

[1] J. Vidal, R. Mosseri, and B. Douçot, Phys. Rev. Lett. **81**, 5888 (1998).
[2] Y. Aharonov, and D. Bohm Phys. Rev. **115**, 485 (1959).
[3] P.W. Anderson, Phys. Rev. **109**, 1492 (1958).
[4] J. Vidal, P. Butaud, B. Douçot, and R. Mosseri, Phys. Rev. B **64**, 155306 (2001)
[5] J. Vidal, B. Douçot, R. Mosseri, and P. Butaud, Phys. Rev. Lett. **85**, 3906 (2000).
[6] J. Vidal, G. Montambaux, and B. Douçot, Phys. Rev. B **62**, R16294 (2000).
[7] S. E. Korshunov, Phys. Rev. B **63**, 134503 (2001).
[8] V. Cataudella and R. Fazio, Europhys. Lett. **61**, 341 (2003).
[9] C.C. Abilio, P. Butaud, T. Fournier, B. Pannetier, J. Vidal, S. Tedesco, and B. Dalzotto, Phys. Rev. Lett. **83**, 5102 (1999).
[10] C. Naud, G. Faini, and D. Mailly, Phys. Rev. Lett. **86**, 5104 (2001).
[11] Y. Aharonov and A. Casher, Phys. Rev. Lett. **53**, 319 (1984).
[12] H. Mathur, and A. D. Stone, Phys. Rev. Lett. **6**8, 2964 (1992)
[13] A.V. Balatsky, and B. L. Altshuler, Phys. Rev. Lett. **70** 1678 (1993).
[14] A. G. Aronov and Y. B. Lyanda-Geller, Phys. Rev. Lett. **70**, 343 (1993).
[15] J. Splettstößer, M. Governale, and U. Zülicke, Phys. Rev. B **68**, 165341 (2003).
[16] D. Frustaglia and K. Richter, Phys. Rev. B **69**, 235310 (2004).
[17] E.I. Rashba, Fiz. Tverd. Tela (Leningrad) **2**, 1224 (1960), [Sov. Phys. Solid State 2, 1109 (1960)].
[18] Y.A. Bychkov and E.I. Rashba, J. Phys. C **17**, 6039 (1984).
[19] J. Nitta, T. Akazaki, H. Takayanagi and T. Enoki, Phys.

Rev. Lett. **78**, 1335 (1997).
[20] T. Schäpers, J. Engels, T. Klocke, M. Hollfelder and H. Lüth, J. Appl. Phys.**83**, 4324 (1998).
[21] D. Grundler, Phys. Rev. Lett. **84**, 6074 (2000).
[22] T. Schäpers, J. Knobbe, and V.A. Guzenko, Phys. Rev. B **69**, 235323 (2004).
[23] J.B. Miller, D.M. Zumbühl, C.M. Marcus, Y.B. Lyanda-Geller, D. Goldhaber-Gordon, K. Campman, and A.C. Gossard, Phys. Rev. Lett. **90**, 76807 (2003).
[24] D. Bercioux, M. Governale, V. Cataudella, and V. M. Ramaglia, Phys. Rev. Lett. **93**, 56802 (2004).
[25] The term in $k_{\rm SO}^2$ can be neglected in realistic situations.
[26] T. Kottos and U. Smilansky, Ann. Phys. (N.Y.) **274**, 76 (1999).
[27] R. Landauer, IBM J. Res. Dev. **1**, 223 (1957).
[28] M. Buttiker, IBM J. Res. Dev. **32**, 317 (1988).
[29] B. Altshuler, A. G. Aronov and B. Spivak, Pis'ma Zh. Eksp. Teor. Fiz. **33**, 101 (1981), [JEPT Lett. **33**, 94, (1981)].
[30] An analysis of edge-state formation in the $\mathcal{T}_3$ lattice can be found in Ref. 4.